Thermoelectric properties of the doped Kondo insulator: $Nd_xCe_{3-x}Pt_3Sb_4$

C. D. W. Jones, K. A. Regan, and F. J. DiSalvo*
Department of Chemistry, Baker Laboratory, Cornell University, Ithaca, New York 14853
(Received 20 July 1998)

The temperature dependence of the thermopower, electrical resistivity, and thermal conductivity were explored for the solid solution $Nd_xCe_{3-x}Pt_3Sb_4$ obtained from the parent Kondo insulator $Ce_3Pt_3Sb_4$. While $Ce_3Pt_3Sb_4$ is a semiconductor with a small activation energy ($E_a \approx 0.05 \pm 0.01$ eV) and a relatively large thermopower ($S = 112 \pm 4$ μV/K at 300 K), $Nd_3Pt_3Sb_4$ is a simple metal with a typically low thermopower ($S = 8 \pm 1$ μV/K at 300 K). The thermoelectric figure of merit ZT of the $Nd_xCe_{3-x}Pt_3Sb_4$ solid solution was found to be maximized at $x = 0.35 \pm 0.10$. The maximum ZT of 0.12 at approximately 230 K, however, is too small to be useful in thermoelectric applications. [S0163-1829(98)05044-9]

I. INTRODUCTION

Most cerium intermediate valence (IV) compounds are metals, with features in the electrical resistivities ρ that can be attributed to the IV behavior.[1] Perhaps the most well-studied cerium IV compound is $CePd_3$. The resistivity is atypical for a simple metal: $\rho(300\ \mathrm{K}) \approx 120$ $\mu\Omega$ cm and $\rho(T)$ has a broad peak ~ 170 $\mu\Omega$ cm centered at approximately 120 K.[2–5] Similarly, a broad but weak peak in the magnetic susceptibility χ is observed in the same temperature range.[4,6,7] $Ce_3Pt_3Sb_4$ has been shown by magnetic susceptibility to be an IV compound with a broad peak in χ at around 400 K.[8–10] In $Ce_3Pt_3Sb_4$, however, the electronic resistivity clearly shows semiconducting behavior with $\rho(300\ \mathrm{K}) \approx 4$ mΩ cm (Refs. 10 and 11) and an estimated activation energy across the gap of ~ 500 K.[8,10,11] To have both IV and semiconducting behavior in a rare-earth (RE) or actinide intermetallic is rare, and these types of compounds are often referred to as Kondo insulators.[12] It should be noted that $CePd_3$ has also been described as a lightly doped Kondo insulator,[13] but the low magnitude of the resistivity (<200 $\mu\Omega$ cm for all $T < 300$ K) leads to this compound more often being referred to as a metal.

Recently, it has been suggested that cerium IV compounds may be a possible source of thermoelectric materials for Peltier cooling applications.[14–16] Often in cerium IV materials, the thermoelectric power (thermopower or Seebeck coefficient) is enhanced over that of regular metals. The IV compounds can have maximal thermopower values around 20–120 μV/K at temperatures below 300 K.[1,17] For example, the thermopower of $CePd_3$ reaches a maximum of 100 ± 20 μV/K at approximately 120 K.[14,18–20] Narrow-band-gap semiconductors have been known for some time to have good thermoelectric properties and chemically substituted Bi_2Te_3 alloys, $(Bi,Sb)_2(Te,Se)_3$, are currently the materials used in Peltier cooling technology.[16,21] Bi_2Te_3 alloys typically have a room-temperature thermopower of about 220 μV/K that decreases as the temperature is lowered.[21] Since $Ce_3Pt_3Sb_4$ shows both IV and small band-gap semiconducting behavior, we thought it might be interesting to evaluate and investigate optimizing this compound as a potential thermoelectric material. Recently, an isostructural compound $Ce_3Cu_3Sb_4$ has also been investigated for its potential thermoelectric properties.[22] This compound also has a semiconducting electrical resistivity, however, the cerium is in a normal Ce^{3+} valence state. To the authors knowledge, the thermopower of the Kondo insulator $Ce_3Pt_3Sb_4$ has not been previously reported, but we show here that it does display significantly large values.

The performance of a thermoelectric material, however, depends on more than just the magnitude of the thermopower. A thermoelectric material is generally characterized by a figure of merit Z, or a dimensionless figure of merit ZT,

$$ZT = \frac{S^2 T}{\rho \kappa}, \tag{1}$$

where T is the temperature, S is the thermopower, ρ is the electrical resistivity, and κ is the thermal conductivity. The efficiency of a thermoelectric device increases with increasing ZT. Optimized Bi_2Te_3 alloys have $ZT \approx 1.0$ near room temperature, however, the ZT decreases steadily as T is lowered.[16,21] Of the cerium IV materials, $CePd_3$ has one of the largest room-temperature ZT values ~ 0.2, which remains roughly constant from 300 to 180 K.[20,23] Attempts at chemically modifying $CePd_3$, however, have not yielded significantly higher S or ZT values.[20,24,25]

In the case of $Ce_3Pt_3Sb_4$, we determine that the ZT values below room temperature are relatively small (<0.07) because of the exponentially increasing electrical resistivity. It was hoped that by doping $Ce_3Pt_3Sb_4$ in some manner, the electrical resistivity would decrease while maintaining the large thermopower of $Ce_3Pt_3Sb_4$. Assuming the thermal conductivity remained unchanged, this would increase the ZT. In $Ce_3Pt_3Sb_4$, chemical substitution can be seen as both the doping of a semiconductor and as modifying the chemical environment around the IV cerium atoms. The IV state is generally quite sensitive to chemical substitutions. By studying the $Nd_xCe_{3-x}Pt_3Sb_4$ system, the near-neighbor environment about any given Ce atom remains unchanged (see Fig. 1). In addition, the metallic radii of Nd (1.814 Å) and Ce (1.818 Å) are similar[26] so the unit cell size would not be dramatically affected. It was thought that both of these factors would help maintain the IV behavior. Although

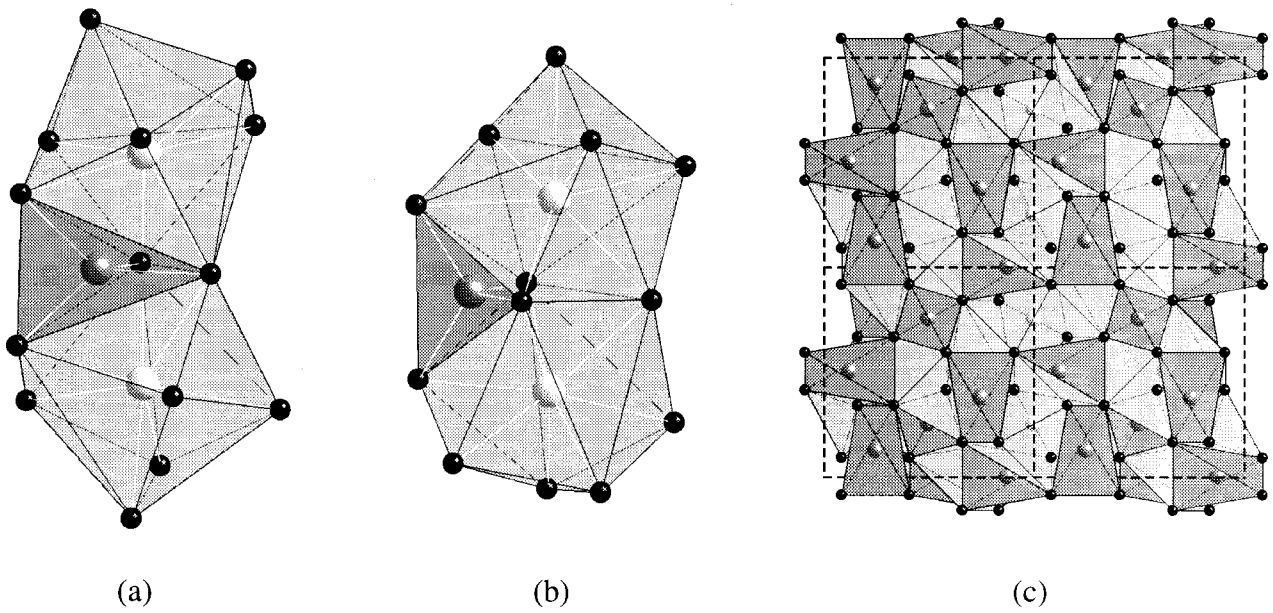

FIG. 1. The main building blocks of the $Ce_3Pt_3Sb_4$ structure are polyhedra with the metal atoms (Pt or Ce) at the center and antimony atoms (shown in black) at the vertices. The Pt atoms (dark gray) are in distorted tetrahedral coordination and the Ce atoms (light gray) are in distorted dodecahedral (bisdisphenoid) coordination. The polyhedral are connected in two configurations (a) with edge-sharing Ce polyhedra and (b) with face-sharing Ce polyhedra. These Ce and Pt polyhedra are arranged to fill all space in the cubic unit cell; four cells are shown in (c).

$Nd_3Pt_3Sb_4$ had not been previously reported, the $Pr_3Pt_3Sb_4$ compound was known to exist and to display metallic behavior.[8] It was thought that the Nd compound would also be metallic and thus, with increasing Nd concentration, help lower the resistivity in the $Nd_xCe_{3-x}Pt_3Sb_4$ compounds.

II. EXPERIMENT

A. Sample preparation

Prior to sample preparation, cerium (Cerac, 12-mm pieces, 99.9%) and neodymium (Cerac, 12-mm pieces, 99.9%) were drip melted under vacuum in a RF furnace to remove any oxide coatings.[27] The pure and unreacted rare earth (RE) metals were then handled only in an inert argon atmosphere. The samples of $Nd_xCe_{3-x}Pt_3Sb_4$ were prepared by arc melting the purified rare earths with the corresponding amounts of platinum (Engelhard, 0.38-mm-diameter wire, 99.99%) and antimony (Cerac, 1–3-mm shot, 99.999%) under a titanium-gettered argon atmosphere. Because of the high vapor pressure of Sb in the synthesis, approximately 1–2 % excess Sb was added for each sample. Each sample was flipped and remelted several times until the mass of the sample (typically ~1 g) was within ±1% of the stoichiometric mass. All the samples were wrapped in tantalum foil, sealed in evacuated silica tubes and annealed at 850 °C for 96 h. The samples were shaped into rectangular bars with approximate dimensions $3\times3\times7\ mm^3$ by cutting with a diamond-impregnated string saw. After cutting, the extra pieces of each sample were ground and analyzed by powder x-ray diffraction (Scintag θ-2θ diffractometer with Cu Kα radiation). Some samples contained trace amounts of RESb and REPtSb second phases (<2% by peak height in the powder x-ray diffraction pattern). The lattice constants obtained from a least-square fitting of the powder diffraction data are shown in Fig. 2.

Overall, $Ce_3Pt_3Sb_4$, is a difficult compound to synthesize because it is incongruently melting and CePtSb is often present as an impurity. The annealing time and temperature were critical in obtaining predominantly single-phase material from the arc-melted samples. A pressed pellet synthesis was also attempted for $Ce_3Pt_3Sb_4$. Stoichiometric amounts of CePt, arc melted and then ground to a powder, and elemental Sb were placed in a vitreous carbon crucible, sealed in an evacuated silica tube, and heated at 950 °C for 48 h. The resulting mixture was ground, pressed into a 0.8 cm diameter pellet, and heated again at 950 °C for 48 h. X-ray powder diffraction of this compound showed the majority phase to be $Ce_3Pt_3Sb_4$, however, there was ~7% CePtSb impurity (based on peak heights in the powder x-ray diffraction pattern). In addition, although the pressed pellet sample integrity was good, it was not as mechanically strong as that of the arc-melted sample. There were also grain boundary ef-

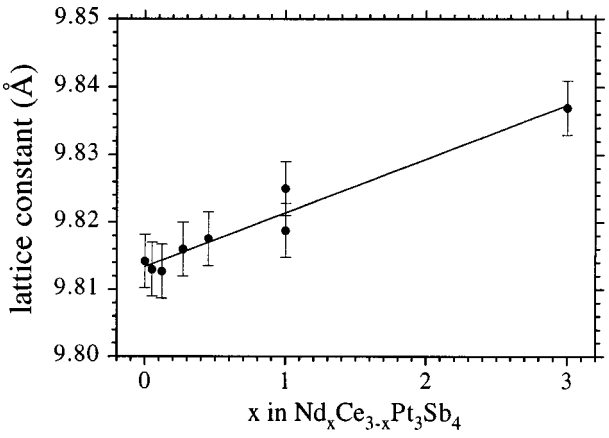

FIG. 2. The cubic lattice constants of the $Nd_xCe_{3-x}Pt_3Sb_4$ series (the line is only shown as a guide to the eye).

fects in the transport property measurements of the pressed pellet (as discussed below). For these reasons, the arc-melting synthesis was chosen for the $Nd_xCe_{3-x}Pt_3Sb_4$ series studied here.

It should be noted that in studying doping in the $Ce_3Pt_3Sb_4$ compound, substitutions of Te, Sn, and Pb were also attempted on the Sb site: $Ce_3Pt_3Sb_{4-y}M_y$, where $y=0.2$ and 1.0 for Te, $y=0.2$ and 0.5 for Sn, and $y=0.7$ and 1.0 for Pb. Both sintered pressed pellets ($M=$Te, Pb) and arc-melted samples ($M=$Sn, Pb) were prepared. These substitutions, however, yielded multiphase compounds ($M=$Te) or predominantly CePtSn or CePtPb, rather than the desired $Ce_3Pt_3Sb_4$-type structure. Attempts at synthesizing $Ce_3Pt_3As_4$ and $Ce_3Pt_3Pb_4$ also yielded predominantly CePtAs or CePtPb.

B. Property measurements

The electrical resistivities were measured on a home-built apparatus using typical four-probe ac techniques. Current contacts to the ends of each sample were made with ultrasonic indium and 0.05-mm-thick copper foil strips. Voltage leads were made by laying 34 AWG copper wires coated with silver epoxy (H20E, Epoxy Technology) onto a flat face of each bar. The absolute value of the resistivity for each sample could vary by $\pm 10\%$ due to uncertainties in the measurement of the area factors.

The thermopower and thermal conductivity were measured simultaneously on each sample using the steady-state technique in another home-built apparatus. Each sample was initially mounted on a copper base with indium solder. A 5-kΩ resistor (heater) was attached to the opposite end of the sample with indium solder. Two 40 AWG Au,Fe(0.07%):Chromel-*p* thermocouples were placed in the indium joints at either end of the sample. After achieving temperature equilibrium, the sample chamber was evacuated to less than 4×10^{-5} Torr. Small, steady temperature gradients (maximum $\sim$2 K) were obtained by incrementally increasing the power to the resistor and the resulting temperatures on either side of the sample were measured. The voltage across the sample was also measured using the Chromel-*p* wires of the two thermocouples. A plot of this voltage versus the temperature gradient gave a slope equal to the thermopower of the sample plus the thermopower of the Chromel-*p* wire. The absolute thermopower of the Chromel-*p* wire was subtracted from the measured slope (thermopower of Chromel-*p* versus Pt from Ref. 28 and absolute thermopower of Pt from Ref. 29). The overall accuracy of the thermopower measurement has been estimated from standards to be within $\pm 5\%$. Another plot of the power to the resistor, divided by the area factor of the sample, versus the temperature gradient gave a slope equal to the thermal conductivity of the sample. The overall accuracy of the thermal conductivity measurement has been estimated from standards of similar dimensions and thermal conductivity to those measured here to be $\pm 15\%$.

III. RESULTS AND DISCUSSION

Although the metallic radii of Nd is nominally smaller than that of Ce,[26] Fig. 2 shows that the lattice parameters actually increase with increasing Nd concentration. This trend results from the unusually small lattice constant of $Ce_3Pt_3Sb_4$ due to the IV state of the cerium. Overall, the difference in lattice parameter between $Ce_3Pt_3Sb_4$ and $Nd_3Pt_3Sb_4$ is small: 0.023(6) Å. This should help maintain the IV state of the cerium.

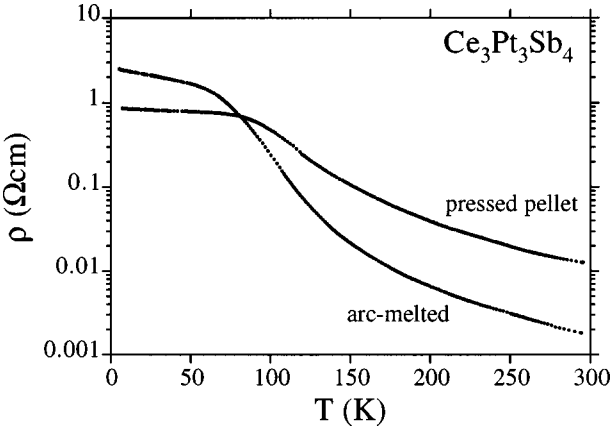

FIG. 3. The electrical resistivity of $Ce_3Pt_3Sb_4$ versus temperature for both a sintered pressed pellet and an annealed arc-melted sample. The room-temperature resistivities differ by almost an order of magnitude.

The semiconducting resistivities of $Ce_3Pt_3Sb_4$, for a sintered pressed pellet and an arc-melted sample, are shown in Figs. 3 and 4. The resistivity for a sintered pressed pellet with $\rho(300\ \mathrm{K})\approx 13\ \mathrm{m\Omega\ cm}$ has been reported previously[8] and matches well with the data here. Other sintered samples have been previously reported with $\rho(300\ \mathrm{K})\approx 4\ \mathrm{m\Omega\ cm}$.[10] This value matches more closely with the arc-melted sample in Figs. 3 and 4 [$\rho(300\ \mathrm{K})\approx 1.8\ \mathrm{m\Omega\ cm}$] but suggests that perhaps grain-boundary scattering and interparticle contact resistance are important in the sintered samples. The concentration of the minor impurities (RESb and REPtSb) might also contribute to differences in the magnitudes of the resistivities. In Fig. 4, the resistivities are plotted on a logarithmic scale versus $1/T$ and show reasonably linear behavior at high temperatures. This linear region can be modeled with the following formula:

$$\rho=\rho_0\exp\left(\frac{E_a}{k_BT}\right). \tag{2}$$

Fitting the arc-melted sample data from 100–300 K gives an activation energy E_a of 734 K. The pressed pellet data, from 150–300 K, yield an E_a value of 635 K. These values are a little higher than previously reported values of 455 K (Ref. 8), 500 K (Ref. 11), and 540 K (Ref. 10) from similar resistivity fits. The E_a of $Ce_3Pt_3Sb_4$ has also been estimated from Hall-effect measurements to be $\sim$1228 K.[10] Similar to the data here, all the reported resistivities show a deviation from simple activated behavior below 100 K; it has been suggested that the behavior below 100 K is dependent on impurities.[8] As Nd is substituted into $Ce_3Pt_3Sb_4$ the magnitude of the resistivity drops significantly (Figs. 5 and 6), and the temperature dependence changes from semiconduct-

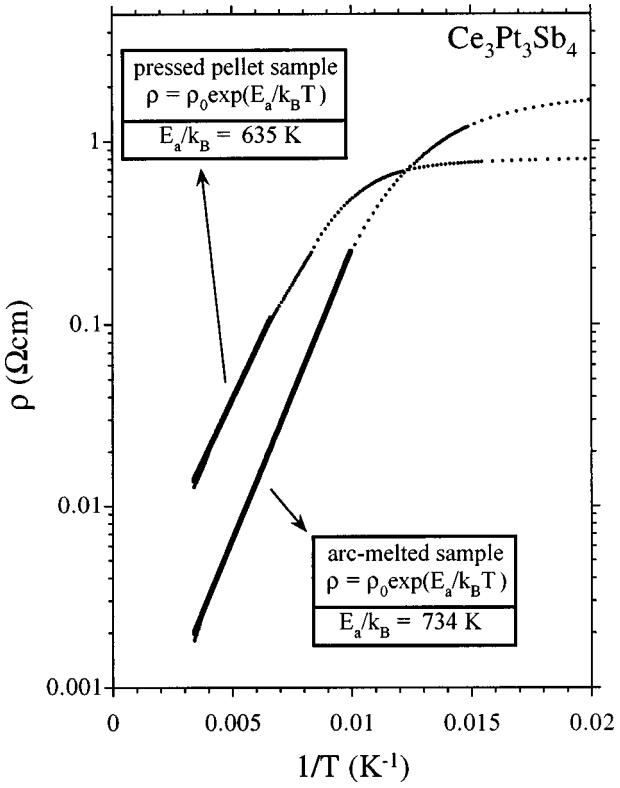

FIG. 4. The electrical resistivity of $Ce_3Pt_3Sb_4$ (on a logarithmic scale) versus 1/T for both a sintered pressed pellet and an annealed arc-melted sample. The high-temperature data agree well with the fit: $\rho = \rho_0 \exp(E_a/k_BT)$. The arc-melted sample data were fit from 100 to 300 K and the pressed pellet data from 150 to 300 K.

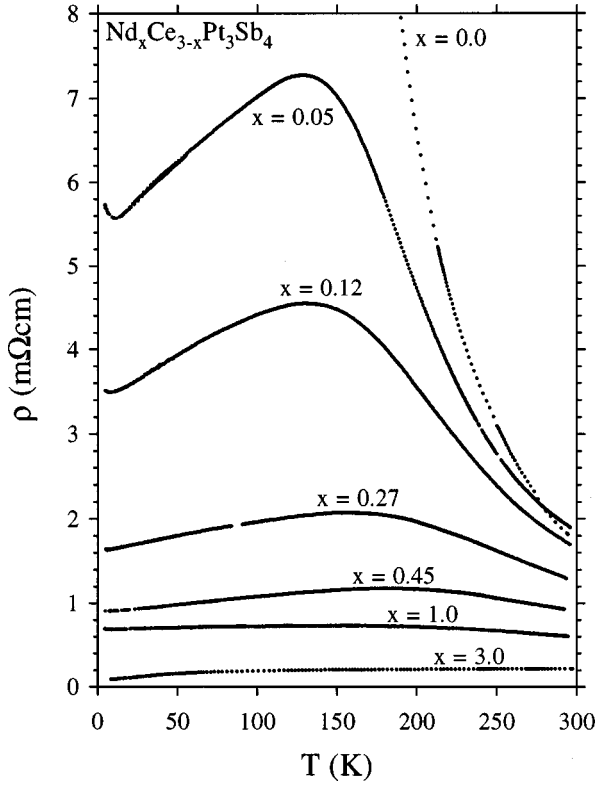

FIG. 5. The electrical resistivities of the $Nd_xCe_{3-x}Pt_3Sb_4$ series versus temperature.

ing to resembling those of IV metallic compounds such as $CePd_3$. The magnitude of the resistivities here, however, are larger than that of $CePd_3$ where the maxima is ~170 $\mu\Omega$ cm at approximately 120 K.[2–5,24] The $Nd_3Pt_3Sb_4$ compound shows metallic type resistivity with a broad rollover near 100 K, probably due to crystal-field effects (Fig. 6). This resistivity is similar in shape to that for a sintered pressed pellet of $Pr_3Pt_3Sb_4$.[8]

The thermopower of $Ce_3Pt_3Sb_4$ is shown in Fig. 7, again for an arc-melted sample and a pressed pellet. Unlike the resistivities, the room-temperature thermopower values are roughly equal, but start to deviate as the temperature is lowered. These differences may again be attributed to different concentrations of impurities or grain-boundary effects in the sintered pressed pellets. The overall shape of these thermopower curves, however, are similar with a large peak at 130 ± 15 K. This again resembles the thermopower of other IV materials like $CePd_3$, which has a maximum of 100 ± 20 μV/K at ~120 K.[14,18–20] The magnitude of the thermopower is certainly larger than the isostructural Kondo insulator $Ce_3Pt_3Bi_4$, which has $S(300\,\text{K}) \approx 10$ μV/K and a peak $S(25\,\text{K}) \approx 70$ μV/K.[30] The temperature dependence of the thermopower is also much different than the isostructural normal valence compound, $Ce_3Cu_3Sb_4$, which has a roughly linear thermopower as a function of temperature.[22,31] The $Nd_3Pt_3Sb_4$ compound, however, shows typical metallic thermopower values (Fig. 8). Thus, as Nd is introduced into $Ce_3Pt_3Sb_4$, the thermopowers drop in magnitude but still show an overall temperature dependence similar to IV-type behavior (Fig. 8).

Figure 9 shows the thermal conductivity of the samples. The thermal conductivity κ is comprised of two components: $\kappa = \kappa_{el} + \kappa_{ph}$. Here, κ_{el} is the contribution from the electronic carriers (holes and electrons) and κ_{ph} is the contribution from the phonon modes (lattice component). In metals, the κ_{el} term generally dominates κ. Since the compounds across the $Nd_xCe_{3-x}Pt_3Sb_4$ series have such different electrical resistivities (carrier densities), one might expect the thermal conductivities to vary greatly as well. In fact, however,

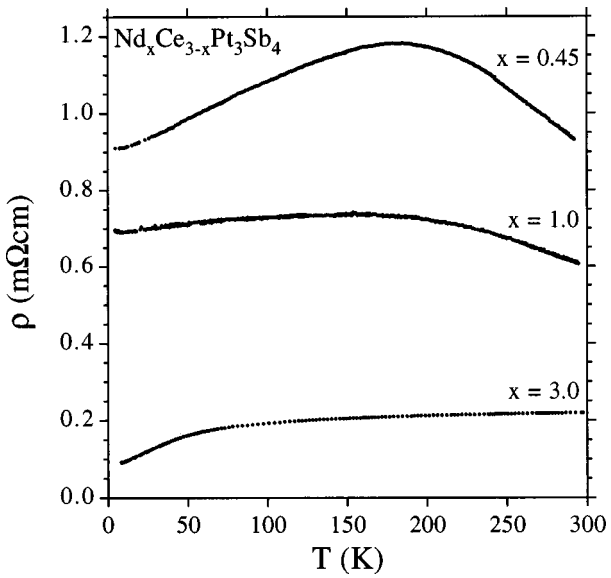

FIG. 6. A selection of the electrical resistivities shown in Fig. 5. Note the metallic resistivity of the $Nd_3Pt_3Sb_4$ compound.

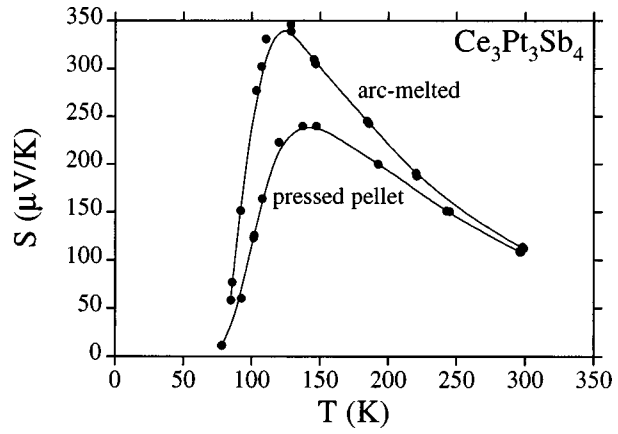

FIG. 7. The thermopower S of $Ce_3Pt_3Sb_4$ versus temperature for both a sintered pressed pellet and an annealed arc-melted sample. Note the similar room-temperature values but the large difference at the peak value. The lines are shown only as a guide to the eye.

the thermal conductivities are all reasonably similar, with only the $Ce_3Pt_3Sb_4$ compound deviating from the series at low temperatures. The room-temperature value for $Nd_3Pt_3Sb_4$ is slightly higher than for $Ce_3Pt_3Sb_4$, in agreement with the larger room-temperature resistivity for $Ce_3Pt_3Sb_4$. As disorder is introduced from the substitution with Nd, one would expect the phonon contribution to the thermal conductivity to be reduced. This seems to be observed with the smaller concentrations of Nd ($x=0.12$ and 0.27) which have

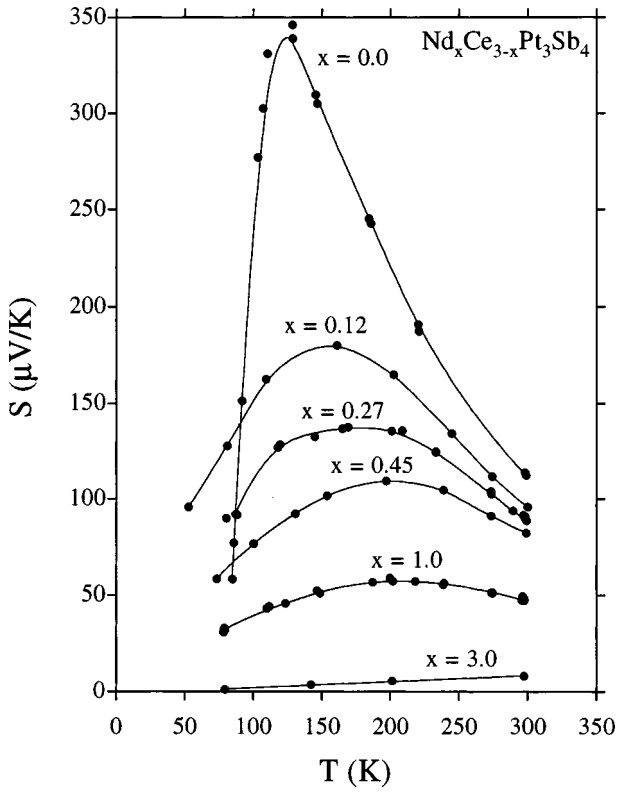

FIG. 8. The thermopower S of the $Nd_xCe_{3-x}Pt_3Sb_4$ series versus temperature. The lines are shown only as a guide to the eye.

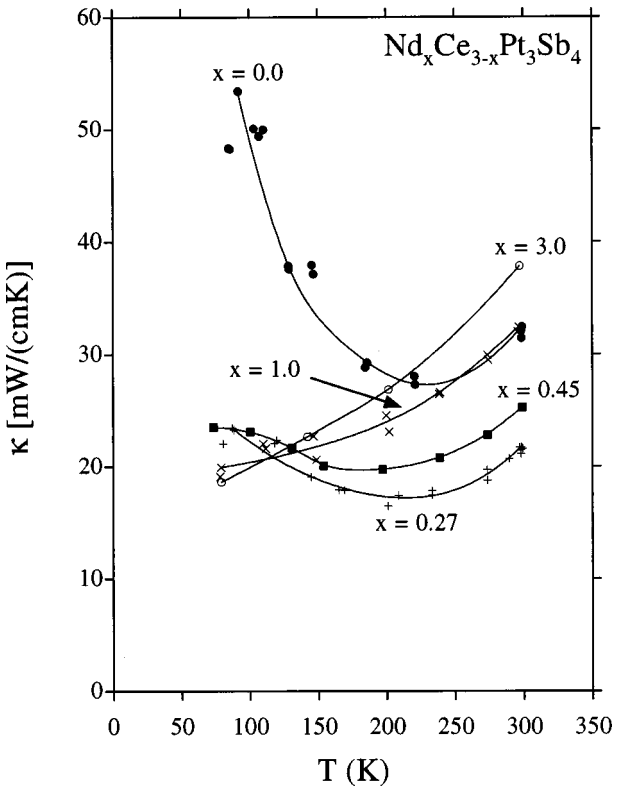

FIG. 9. The thermal conductivity κ of the $Nd_xCe_{3-x}Pt_3Sb_4$ series versus temperature. The $x=0.12$ data overlaps the $x=0.45$ data over the whole temperature range and has been omitted for clarity. The lines are shown only as a guide to the eye.

much smaller κ at low temperature in comparison to $Ce_3Pt_3Sb_4$. The minimum value of $\kappa \approx 17$ mW/cm K is equal to those typically found in the Bi_2Te_3 alloys.[21] As the amount of Nd increases, however, the κ_{el} becomes more important and the total κ increases. Overall, the values measured here are similar to those for polycrystalline samples of the isostructural normal valence compound $Ce_3Cu_3Sb_4$.[22] It should be noted that thermal conductivity is a difficult property to measure accurately and makes interpretation of the small differences in κ problematic.

Another way to represent the thermal conductivity data is to look at the Lorentz number ($L=\rho\kappa/T$, where as defined here, the κ is the total thermal conductivity). As previously mentioned, for typical metals, the thermal conductivity is dominated by the electronic component. In this case, the Wiedemann-Franz law is valid and the Lorentz number will equal

$$L_0=\frac{\pi^2}{3}\left(\frac{k_B}{e}\right)^2=2.44\times10^{-8}\ (\mathrm{V/K})^2. \tag{3}$$

$L/L_0>1$ suggests that the phonon contribution to the thermal conductivity is important. The L/L_0 values for the $Nd_xCe_{3-x}Pt_3Sb_4$ series are shown in Fig. 10 on a logarithmic scale. For $Nd_3Pt_3Sb_4$, the L/L_0 values are ~ 1, again suggesting typical metallic behavior. $Ce_3Pt_3Sb_4$, however, has extremely large L/L_0 values suggesting that the thermal conductivity is dominated by phonons. As Nd is introduced into

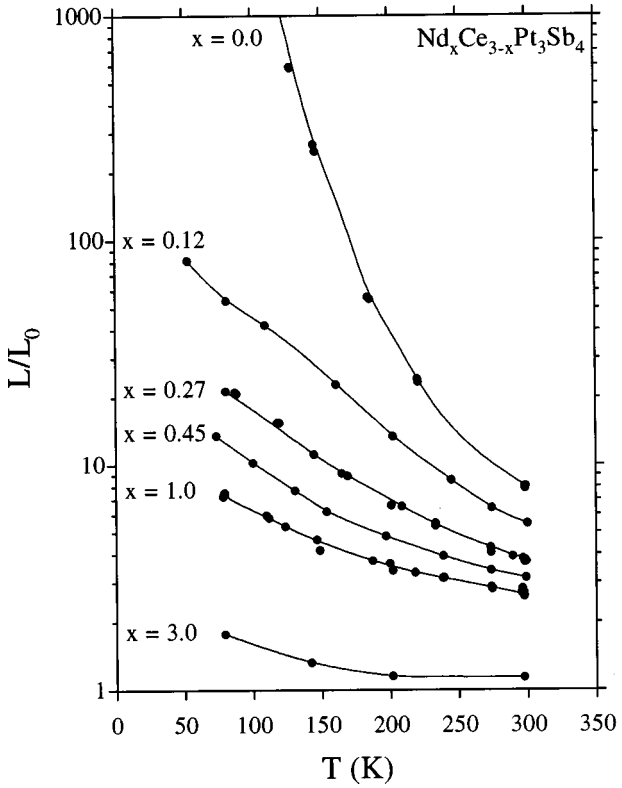

FIG. 10. The Lorentz ratio L/L_0 for the $Nd_xCe_{3-x}Pt_3Sb_4$ series (on a logarithmic scale) versus temperature. The lines, shown only as a guide to the eye, suggest that L/L_0 is increasing almost exponentially as the temperature is lowered.

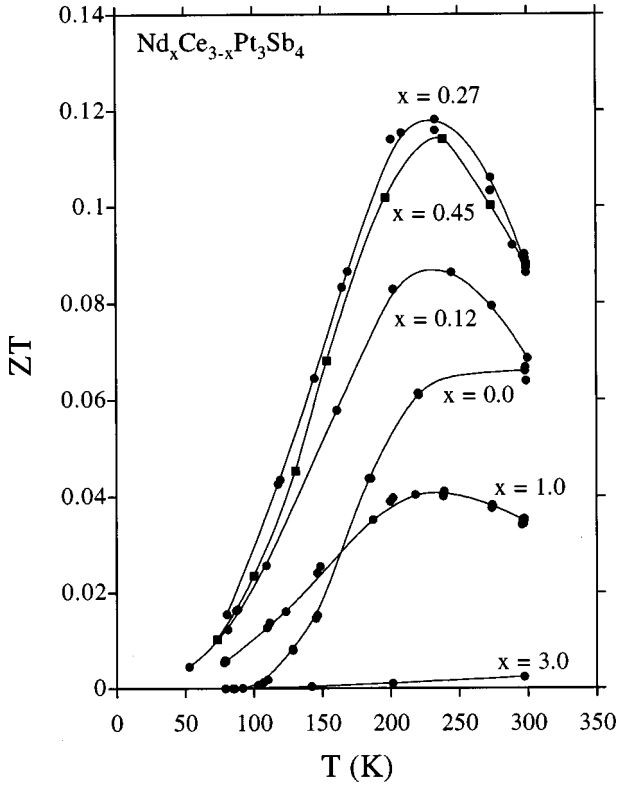

FIG. 11. The thermoelectric figure of merit ZT versus temperature for the $Nd_xCe_{3-x}Pt_3Sb_4$ series. Note that the ZT of $Ce_3Pt_3Sb_4$ is improved for small substitutions of Nd ($x=0.27$ and 0.45). The lines are shown only as a guide to the eye.

$Ce_3Pt_3Sb_4$, the L/L_0 values decrease dramatically. For any given compound, the L/L_0 values increase rapidly, almost exponentially, as the temperature is lowered, thus looking reasonably linear in Fig. 10. As the temperature decreases, the contribution from the phonon component to the thermal conductivity seems to become relatively more important. However, it should be noted that the IV metal $CePd_3$ (Refs. 3 and 20) and the heavy fermion compound $CeCu_6$ (Ref. 32) also show an increase in L/L_0 as the temperature decreases. It is possible that another mechanism, perhaps related to valence fluctuation, is contributing to these rises in L/L_0 as a function of decreasing temperature.

Finally, the ZT curves in Fig. 11 show that an increase in ZT is possible with Nd substitution in $Ce_3Pt_3Sb_4$. The maximum values of ZT are found near 230 ± 10 K for most of the compounds and a plot of ZT (230 ± 10 K) versus Nd concentration is shown in Fig. 12. The maximum ZT value of 0.12 is roughly double that of the pure $Ce_3Pt_3Sb_4$ compound, but certainly still too small for any potential thermoelectric applications. The peaks in ZT versus T here are also smaller, and much sharper than, the relatively flat region of $ZT\approx0.2$ from 180 to 300 K in $CePd_3$.[20,23] Perhaps other substitutions in this compound, such as other transition metals on the Pt site, may yield other interesting changes in the ZT characteristics of these materials. Other Kondo-insulating compounds,[12] such as the filled skutterudite material $CeFe_4P_{12}$, might also be interesting to pursue as low-temperature thermoelectric materials.

IV. CONCLUSIONS

The solid solution between the semiconducting Kondo insulator $Ce_3Pt_3Sb_4$ and the normal metal $Nd_3Pt_3Sb_4$ has yielded compounds that show intermediate valence-type resistivities. The thermopower of $Ce_3Pt_3Sb_4$ was found to be significant with $S=112\pm4\ \mu$V/K at 300 K and up to $343\pm10\ \mu$V/K at 128 K, much larger than the isostructural $Ce_3Pt_3Bi_4$.[30] Although the thermopower decreases with Nd substitution into $Ce_3Pt_3Sb_4$, the thermoelectric figure of merit is increased for intermediate concentrations of Nd,

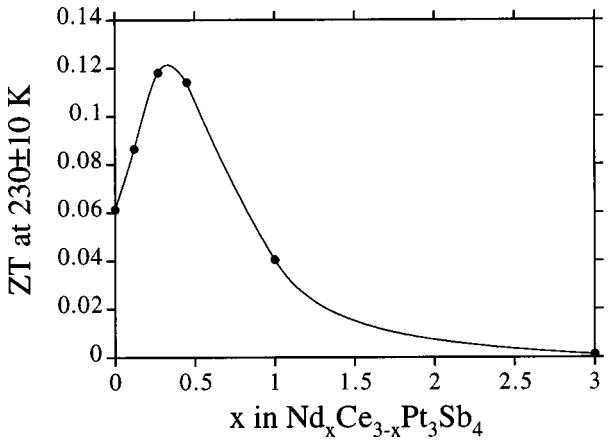

FIG. 12. The thermoelectric figure of merit ZT at 230 ± 10 K versus Nd concentration. The line is shown only as a guide to the eye but suggests that the maximum ZT occurs at $x=0.35\pm0.10$.

reaching a maximum at $x = 0.35 \pm 0.10$ in $Nd_xCe_{3-x}Pt_3Sb_4$. The maximum *ZT* of 0.12 at approximately 230 K, however, is too small to be useful in thermoelectric applications. It does show that Kondo insulator compounds may have potential as thermoelectric materials if the appropriate doping schemes can be developed.

ACKNOWLEDGMENTS

The authors would like to thank K. J. Proctor for his assistance in designing and testing the thermopower apparatus. This research was funded by the Office of Naval Research. C.D.W.J. would also like to thank the Natural Sciences and Engineering Research Council of Canada for support.

*Author to whom correspondence should be addressed. FAX: 607-255-4137. Electronic address: fjd3@cornell.edu

[1] J. M. Lawrence, P. S. Riseborough, and R. D. Parks, Rep. Prog. Phys. **44**, 1 (1981).
[2] P. Scorbia, J. E. Crow, and T. Mihalisin, J. Appl. Phys. **50**, 1895 (1979).
[3] H. Schneider and D. Wohlleben, Z. Phys. B **44**, 193 (1981).
[4] J. R. Thompson, S. T. Seula, C.-K. Loong, and C. Stassis, J. Appl. Phys. **53**, 7893 (1982).
[5] D. Müller, S. Hussain, E. Cattaneo, H. Schneider, W. Schlabitz, and D. Wohlleben, in *Valence Instabilities*, edited by P. Wachter and H. Boppart (North-Holland, Amsterdam, 1982), p. 463.
[6] W. E. Gardner, J. Penfold, T. F. Smith, and I. R. Harris, J. Phys. F **2**, 133 (1972).
[7] P. A. Veenhuizen, Y. Fu-ming, H. van Nassou, and F. R. de Boer, J. Magn. Magn. Mater. **63&64**, 567 (1987).
[8] M. Kasaya, K. Katoh, and K. Takegahara, Solid State Commun. **78**, 797 (1991).
[9] K. Katoh and M. Kasaya, Physica B **186-188**, 428 (1993).
[10] K. Katoh and M. Kasaya, J. Phys. Soc. Jpn. **65**, 3654 (1996).
[11] M. Kasaya, K. Katoh, M. Kohgi, T. Osakabe, and N. Sato, Physica B **199&200**, 534 (1994).
[12] G. Aeppli and Z. Fisk, Comments Condens. Matter Phys. **16**, 155 (1992).
[13] B. Bucher, Z. Schlesinger, D. Mandrus, Z. Fisk, J. Sarrao, J. F. DiTusa, C. Oglesby, G. Aeppli, and E. Bucher, Phys. Rev. B **53**, R2948 (1996).
[14] R. J. Gambino, W. D. Grobman, and A. M. Toxen, Appl. Phys. Lett. **22**, 506 (1973).
[15] G. D. Mahan, Bull. Am. Phys. Soc. **41**, 58 (1996).
[16] G. D. Mahan, Solid State Phys. **51**, 81 (1998).
[17] D. Jaccard and J. Sierro, in *Valence Instabilities* (Ref. 5), p. 409.
[18] H. Sthioul, D. Jaccard, and J. Sierro, in *Valence Instabilities* (Ref. 5), p. 443.
[19] M. Houshiar, D. T. Adroja, and B. D. Rainford, Physica B **223&224**, 268 (1996).
[20] K. J. Proctor, C. D. W. Jones, and F. J. DiSalvo (unpublished).
[21] W. M. Yim and F. D. Rosi, Solid-State Electron. **15**, 1121 (1972).
[22] K. Fess, W. Kaefer, Ch. Thurner, K. Friemelt, Ch. Kloc, and E. Bucher, J. Appl. Phys. **83**, 2568 (1998).
[23] G. Mahan, B. Sales, and J. Sharp, Phys. Today **50** (3), 42 (1997).
[24] Y. Ijiri and F. J. DiSalvo, Phys. Rev. B **55**, 1283 (1997).
[25] C. D. W. Jones, R. A. Gordon, B. K. Cho, F. J. DiSalvo, J. S. Kim, and G. R. Stewart (unpublished).
[26] N. N. Greenwood and A. Earnshaw, *Chemistry of the Elements* (Pergamon, New York, 1984), p. 250.
[27] R. A. Gordon, Ph.D. thesis, Cornell University, 1995.
[28] G. W. Burns, M. G. Scroger, G. F. Strouse, M. C. Croarkin, and W. F. Guthrie, NIST Monograph 175, 1993.
[29] C. L. Foiles, in *Numerical Data and Functional Relationships in Science and Technology*, edited by K.-H. Hellwege and J. L. Olsen, Landolt-Börnstein, New Series, Group III, Vol. 15, pt. b (Springer-Verlag, New York, 1985), p. 63.
[30] M. F. Hundley, P. C. Canfield, J. D. Thompson, Z. Fisk, and J. M. Lawrence, Physica B **171**, 254 (1991).
[31] R. V. Skolozdra, P. S. Salamakha, A. L. Ganzyuk, and O. I. Bodak, Inorg. Mater. **29**, 26 (1993).
[32] E. Brück, A. Nowack, N. Hohn, E. Paulus, and A. Freimuth, Z. Phys. B **63**, 155 (1986).